

Standard Sources of Particle Production in Heavy Ion Collisions

A. CAPELLA

Laboratoire de Physique Théorique (CNRS - UMR 8627),
Université de Paris XI, Bâtiment 210, 91405 Orsay Cedex, France

We describe particle production in the framework of an independent string model : the dual parton model. We show that an improved version of this model, containing a diquark breaking component, allows to describe the bulk of particle production and, in particular, baryon stopping and most of the observed enhancement of strange baryons. Only for very rare processes, such as Ω or J/ψ production, the model has to be supplemented with final state interaction (comovers interaction). Recent data on event-by-event fluctuations in p_T are also described by the model. Predictions for RHIC and LHC are presented and the effect of nuclear shadowing is discussed.

LPT-ORSAY 99-75

1. Introduction

The enhanced production of strange particles (in particular of strange baryons) and the spectacular suppression of J/ψ in $PbPb$ collisions are considered by many authors to be signals of Quark Gluon Plasma (QGP) production –or at least of the production of a system in thermal equilibrium. In this paper, we describe these phenomena in the framework of the dual parton model (DPM). We show that the model in its original form fails to describe the large amount of stopping measured in central SS and $PbPb$ collisions –as do most independent string models. An improved version of the model containing a diquark breaking component is introduced. It allows to describe stopping without any extra free parameter. The same component is also responsible for most of the observed enhancement of strange baryons. However, the Ω yield is underestimated by a factor five. Agreement with experiment is restored by introducing final state interaction (comovers interaction) with a very small cross-section of the order of 0.1

mb. Comovers interaction is also needed in order to describe the anomalous suppression of J/ψ in central $PbPb$ collisions.

Comovers interaction is a very non-trivial phenomenon mostly at a partonic level, which is not entirely understood. It turns out, however, that the cross-sections required to describe the data, both for strangeness enhancement and J/ψ suppression are very small and the comovers interaction does not affect the bulk of particle production. In particular $B\bar{B}$ annihilation in the final state seems to be negligibly small.

Recently, a lot of attention has been devoted to the study of event-by-event correlations –in particular in p_T . The small value of this correlation in central $PbPb$ collisions has been interpreted as a sign of thermalization. We show that this value is well reproduced in DPM.

Predictions of the model for RHIC and LHC are also presented. Although minijets are important in order to determine p_T distributions, in DPM they do not affect multiplicities. (For the latter, the short $q\bar{q}$ strings in DPM play the same role as minijets). On the contrary, shadowing corrections are very important and reduce the values of dN/dy at mid-rapidities by a factor 2 at RHIC and by a factor 3 at LHC. This reduction is much stronger than in models where minijets are the dominant component. The reason being that in DPM shadowing corrections are present both for soft and semi-hard production.

2. The model

The dual parton model (DPM) is a dynamical model for low p_T hadronic and nuclear interactions. It is based on the large- N expansion of non-perturbative QCD in the Veneziano limit –in which the ratio N_c/N_f is held fixed [1]. The dominant configuration consists in the production of two strings (of type $qq\bar{q}$ in pp scattering, see Fig. 1). There are also more complicated configurations, corresponding to higher order terms in the large- N expansion, involving 4, 6, ... etc strings. These extra strings have sea quarks and antiquarks at their ends (Fig. 2). These configurations correspond to multiple inelastic scattering in an S -matrix approach. In pp collisions the contribution of each configuration is suppressed by a factor N^{-2n+2} , where n is the number of strings –irrespective of the number of exchanged gluons and $q\bar{q}$ loops, which do not change the topology of the graph. It is not known how to compute the numerical values of the various contributions from the QCD lagrangian. However, Veneziano has shown that there is a one-to-one correspondence between the various terms in the $1/N$ expansion and those in a multiple scattering theory (the number of strings being equal to twice the number of inelastic collisions). In view of that, we determine the contribution of each configuration to the total cross-section using a multiple

scattering model : generalized eikonal or perturbative reggeon calculus in hadron-hadron collisions and Glauber-Gribov model in collisions involving nuclei.

For $A - B$ collisions (for simplicity we consider here $A = B$) in the approximation of only two strings per nucleon-nucleon collisions, the rapidity distribution of secondaries is given by [2]

$$\frac{dN^{AA}}{dy}(y) = \bar{n}_A \left[N^{qq_{A_P} - q_{A_T}^v}(y) + N^{q_{A_P}^v - qq_{A_T}}(y) \right] + 2(\bar{n} - \bar{n}_A)N^{q_s - \bar{q}_s}(y) . \quad (1)$$

Here $N(y)$ are the rapidity distributions of the individual strings, \bar{n}_A is the average number of wounded nucleons of A and \bar{n} is the average number of collisions. Both \bar{n}_A and \bar{n} can be computed in the Glauber model. For instance for an average collision (i.e. integrated over impact parameter), one has

$$\bar{n} = A^2 \sigma_{NN} / \sigma_{AB} \propto A^{4/3} . \quad (2)$$

Note that the total number of strings is $2\bar{n}$, i.e. two strings per inelastic nucleon-nucleon collision.

The interpretation of (1) is obvious. With \bar{n}_A struck nucleons, we have at our disposal \bar{n}_A diquarks of projectile and target (qq_{A_P} and qq_{A_T} , respectively) and as many valence quarks. This accounts for the first term in (1). The remaining strings : $2(\bar{n} - \bar{n}_A)$ have to be stretched by sea quarks and antiquarks, because the available valence constituents are all included in the first term ; this accounts for the second term of (1). Of course we should combine the valence and sea constituents of the projectile with those of the target in all possible ways. However, for linear quantities such as multiplicities, each ordering gives practically the same result.

We can see from (1) and (2) that, if all strings would have the same plateau height (i.e. the same value of $N(0)$), the plateau height in an average AA collision would increase like $A^{4/3}$. However, at present energies, the plateau height of the $q_s - \bar{q}_s$, strings is smaller than that of $qq - q$ ones, and the first term of (1) dominates. One obtains in this way the celebrated wounded nucleon model introduced by our Krakow hosts [3]. At higher energies the contribution of the sea strings becomes increasingly important. Therefore, in order to make predictions for RHIC and LHC we have to introduce the multistring configurations in each nucleon-nucleon collision. If their average number is $2\bar{K}$ (this number can be computed in a generalized eikonal model : one gets $\bar{K} \simeq 2$ at $\sqrt{s} = 200$ and $\bar{K} \approx 3$ at $\sqrt{s} = 7$ TeV) the total number of strings is $2\bar{K}\bar{n}$ and Eq. (1) is changed into

$$\begin{aligned} \frac{dN^{AA}}{dy}(y) = & \bar{n}_A \left[N^{qq_{AP}-q_{AT}^v}(y) + N^{q_{AP}^v-qq_{AT}}(y) + (2\bar{K} - 2)N^{q_s-\bar{q}_s} \right] \\ & + (\bar{n} - \bar{n}_A)2\bar{K}N^{q_s-\bar{q}_s} . \end{aligned} \quad (3)$$

The hadronic spectra of the individual strings $N(y)$ is obtained from a convolution of momentum distribution function and fragmentation functions. Both are assumed to be universal, i.e. the same in all hadronic and nuclear interactions. This makes the model very predictive, in particular regarding the energy and A -dependences. Moreover, momentum distribution functions and fragmentation functions are determined to a large extent from known Regge intercepts [2] [4]. Finally, hadrons produced in different strings are assumed to be uncorrelated (string independence). This is a simplicity assumption which does not follow from the large- N expansion.

So far, we have only considered configurations with an even number of strings. What about odd string configurations. A configuration with a single $3\bar{3}$ string is possible in some cases, i.e. when it is possible to annihilate a projectile quark with the corresponding antiquark in the target (Fig. 3). However, in this case flavor quantum numbers are exchanged between projectile and target and this contribution decreases like $1/\sqrt{s}$ (secondary reggeon exchange).

A configuration with three $3\bar{3}$ strings is possible in $p\bar{p}$ annihilation (Fig. 4). In this case, baryon number is exchanged between projectile and target, and the corresponding contribution is also expected to decrease in $1/\sqrt{s}$. In any case, it is known experimentally that this contribution is very small at high energy.

3. Baryon stopping

In DPM, the net baryon production takes place from diquark fragmentation. The produced baryon is fast in average. The data for pp collisions at SPS and for peripheral AA collisions can be reproduced in this way. However, in the case of central SS and $PbPb$ collisions, a huge baryon stopping has been observed by both the NA44 and NA49 collaborations. It cannot be reproduced in the model. Actually most string models in their original form fail to do so.

The origin of this problem resides in the association of the net baryon production with the diquark. This is not necessarily the case. Indeed, let us consider again the three string graph for $p\bar{p}$ annihilation of Fig. 4. Here the valence quarks and antiquarks are found in their corresponding hemispheres and yet no baryon or antibaryon is present in the final state. This indicates that baryon number can be independent of valence quarks. It also

shows that it can be transferred over large rapidity distances and annihilate with the corresponding antibaryon number –very much in the same way as quark and antiquark annihilate in the one string diagram of Fig. 3. Assuming that $\sigma_{annihilation} \sim 1/\sqrt{s}$, one obtains for the rapidity distribution of baryon number (when it is not associated with valence quarks) $d\sigma/dy \sim \exp(-1/2\Delta y)$.

The above picture has its theoretical justification in the works of Dosch [5] and Rossi and Veneziano [6]. These authors have constructed a gauge invariant state vector of the baryon which leads to a picture of the baryon made out of three quarks bound together by three strings which join in a point called string junction (SJ). In this picture it is possible to transfer the SJ over large rapidity distances –leaving the valence quarks behind. In what follows, this component will be denoted diquark breaking (DB) component - while the conventional one will be denoted diquark preserving (DP) component.

Recent work based on the above or related ideas can be found in Refs. [7]-[13]. However, in order to understand in this way the huge stopping observed in central AA collisions, one has to understand why the DB component described above is small in pp and quite large in central AA collisions. In Ref. [10], it was argued that the A dependence of the DB component is stronger than that of the DP one. In this way, a satisfactory description of the pp and central SS data was obtained –and predictions for central $PbPb$ turned out to be correct. This was achieved by introducing one free parameter –which determines the ratio of the DB over DP contribution in pp . However, this approach is not entirely satisfactory since it requires a sort of fine tuning, namely the size of the DB component in pp has to be small enough not to spoil the agreement with the data, and large enough to describe the central AA data thanks to its larger A dependence.

In recent works [12, 13], we have introduced a different implementation of the DB mechanism which avoids any fine tuning –as well as the necessity of an extra parameter. Our first remark is that, although the DB component is definitely present in the case of a single pp collision, it gives rise to a three-string configuration (Fig. 5). This is not the dominant, two-string, configuration in the large- N expansion and, therefore, is expected to be small. Since its presence is not required to describe the pp data at SPS energies, we take it equal to zero for simplicity. (Actually any value small enough to be in agreement with the pp data can be introduced but it will have practically no effect on the results for central AB collisions). The second important remark [10] is that in the case of two inelastic collisions per nucleon (for instance an incoming proton scattering inelastically with two nucleons of a nuclear target), the above topological suppression does not occur. Indeed, in this case the dominant configuration has four strings

for both the DP and the DB components (see Figs. 2 and 6). Therefore a natural assumption is that, in this case, the two contributions have equal weights (1/2). The generalization to the case of n elastic collisions per nucleon is not so obvious. The assumption we have made [12, 13] (to be checked by comparing with experiment) is that there is an equal probability (1/ n) for the SJ to follow any of the n collisions. In one of them, the SJ will join a valence diquark and hadronize in the conventional (DP) way. In all other cases, it will hadronize according to the DB mechanism.

With these assumptions, the rapidity distribution of the net baryon ($B - \bar{B}$) in AA collisions can be written as

$$\frac{dN^{AA \rightarrow B - \bar{B}}}{dy} = \frac{\bar{n}_A}{\bar{n}} \left[\bar{n}_A \frac{dN_{DP}}{dy} + (\bar{n} - \bar{n}_A) \frac{dN_{DB}}{dy} \right]. \quad (4)$$

Here \bar{n} is the average number of binary collisions and \bar{n}_A the average number of participants of A (for simplicity we consider only the case $A = B$). The average number of collisions per wounded (or participant) nucleon is \bar{n}/\bar{n}_A . The probability of the DP component is thus \bar{n}_A/\bar{n} and that of the DB one $1 - \bar{n}_A/\bar{n} = (\bar{n} - \bar{n}_A)/\bar{n}$. The extra factor \bar{n}_A in Eq. (4) ensures baryon number conservation (see below). Note that in the case of a single collision per nucleon ($\bar{n} = \bar{n}_A$), only the DP component is present. The exact form of dN_{DB}/dy is given in Refs. [12, 13]. Its main feature is the $\exp(-1/2\Delta y)$ factor, discussed above. In Eq. (4), dN_{DP}/dy is the conventional diquark fragmentation component. All relevant formulae are given in Ref. [14]. Both components are normalized to 2 (upon integration in y). In this way, the net baryon yield is $2\bar{n}_A$ as required by baryon number conservation.

Note that in pp collisions at high energy there is also more than one collision per nucleon due to unitarity. Therefore, Eq. (4) gives a well defined prediction for the increase of stopping in hadronic collision at high energies. An obvious prediction is that the stopping will increase with the event multiplicity –large event multiplicity corresponding to a large number of interactions and/or strings. Preliminary data for the $p-\bar{p}$ asymmetry in DIS at HERA are in qualitative agreement with this prediction.

The results for the net baryon yield $B - \bar{B}$ in central SS and $PbPb$ collisions are shown in Fig. 7. The $PbPb$ data are well reproduced. The SS ones (which show a larger stopping than in $PbPb$) are not so well described. Note, however, that the discrepancy between the data and the model predictions without DB component has been substantially reduced. Note also that there is no free parameter here.

4. Strangeness enhancement

We have argued in the previous section that in central AA collisions, a large number of net baryons are produced at mid-rapidities and that they are dominantly made out of the SJ plus three sea quarks (see Fig. 6). It is then obvious than a large number of net Λ , Ξ and Ω (i.e. an increase of these yields per participant) will also take place. As a matter of fact, this is the only possibility to produce net Ω . The experimental value of the ratio $\bar{\Omega}/\Omega \sim 0.4$ in central $PbPb$ collisions at mid-rapidities is very much in favor of the above picture. Moreover, there will also be a substantial increase in the yield of K^+ associated to the production of Λ 's.

In order to obtain the absolute yields of strange baryons one can use trivial quark counting arguments together with the ratio $S = 2s/(u + d)$ of strange over non-strange quarks in the sea. Details of the calculations, using values of S in the range $0.2 \div 0.3$, can be found in ref. [13]. Very similar results are obtained [12] by adopting a more phenomenological attitude, namely, fixing the Λ , Ξ and Ω yields at mid-rapidities from the pBe and pPb data [15]. Their values in central AA collisions are then obtained using Eq. (4).

Before stating our results it is necessary to recall the mechanism of antibaryon production in DPM. It consists of two terms. One of them corresponds to the usual diquark antidiquark pair production in the string breaking process. This term scales with the number of participants. The second one corresponds to the presence of diquark-antidiquark pairs in the nucleon sea. This term scales with $\bar{n} - \bar{n}_A$.

The corresponding formula (for $A = B$) is

$$\frac{dN^{AA \rightarrow \bar{B}}}{dy} = n_A \frac{dN_{string}^{AA \rightarrow \bar{B}}}{dy} + (\bar{n} - \bar{n}_A) \frac{dN_{sea}^{AA \rightarrow \bar{B}}}{dy} . \quad (5)$$

For details see [12, 13] and references therein.

Our results are shown in Fig. 8 (dashed lines). The p and Λ yields are well reproduced. The Ξ 's are slightly underestimated. However, the Ω 's are too low by a factor 5. In an attempt to describe the Ω yield we have introduced the final state interactions : $\pi N \rightarrow K\Lambda$, $\pi N \rightarrow K\Sigma$, $\pi\Lambda \rightarrow K\Xi$, $\pi\Sigma \rightarrow K\Xi$ and $\pi\Xi \rightarrow K\Omega$, plus the corresponding reactions for the antiparticles. They are governed by the gain and loss differential equations [16]

$$\frac{dN_i}{d^4x} = \sum_{K,\ell} \sigma_{k\ell} \rho_k(x) \rho_\ell(x) - \sum_k \sigma_{ik} \rho_i(x) \rho_k(x) . \quad (6)$$

The first term in the r.h.s. of (6) describes the production of particle i resulting from the interaction of particles k and ℓ with space-time densities

$\rho(x)$ and cross-sections $\sigma_{k\ell}$ (averaged over the momentum distributions of the interacting particles. The second term describes the loss of particle i due to its interaction with particle k . The initial densities are the ones obtained without final state interaction and the averaged cross-sections are taken to be the same for all processes. For details see [12, 13]. The data are reproduced with a value of the cross-section as small as 0.14 mb (full lines in Fig. 8). Note that we do not consider the inverse reactions required by detailed balance. These reactions give a negligibly small effect since $\rho_K\rho_\Lambda \ll \rho_\pi\rho_N$, etc. For the same reason we have neglected strange exchange reactions such as $\pi\Omega \leftrightarrow \bar{K}\Xi$. Although the averaged cross-section can be larger than the value used above, this is overcompensated by the values of the involved densities. Since $\rho_\Omega \ll \rho_\Xi$ (by a factor 20 at initial interaction time), $\pi\Omega \rightarrow \bar{K}\Xi$ is disfavored as compared to $\pi\Xi \rightarrow K\Omega$. Likewise, since $\rho_{\bar{K}} \ll \rho_\pi$, $\bar{K}\Xi \rightarrow \pi\Omega$ is disfavored as compared to $\pi\Xi \rightarrow \bar{K}\Omega$.

Note that final state interaction is by no means a trivial effect. First, it represents a departure from the idea of independent strings. Second, and more important, a large contribution to the integrals (6) comes from interaction times of a few fermi, close to initial time where the system is in a dense pre-hadronic state. Actually, Brodsky and Muller [17] introduced the concept of comover interaction as a coalescence phenomenon at the partonic level, in order to describe the final state interaction. It is therefore clear that a lot of theoretical uncertainty is introduced in this way. The important result, however, is that the cross-sections required to describe the data are very small and do not affect the bulk of particle production.

In Fig. 9 we show the ratio \bar{B}/B for pPb and for four centrality bins in $PbPb$. All these ratios decrease significantly between pPb and central SS collisions and also between central SS and central $PbPb$. Although this decrease does not contradict thermal or QGP models (the increase in these ratios at fixed baryochemical potential can be overcompensated by an increase of the latter), it is not easy to obtain and most global fits in the framework of those models do not reproduce it. A more crucial test of the thermal and QGP models is the ratio of different types of antibaryons. An important result of our model is a ratio $\bar{\Lambda}/\bar{p}$ significantly smaller than one. This is in agreement with recent preliminary data on the \bar{p} yield from the NA49 collaboration [18] –together with published data on the $\bar{\Lambda}$ yield by the WA97 one [15]. This is in contradiction with the prediction of a $\bar{\Lambda}/\bar{p}$ ratio significantly larger than one given by J. Rafelski [19].

5. J/ψ suppression

¹ The decrease of the ratio J/ψ over DY when the centrality increases was proposed by Matsui and Satz [20] as a test of a deconfining phase transition. Shortly afterwards this decrease was found in OU collisions by the NA36 collaboration. It has also been found in SU and $PbPb$ –as well as in pA collisions (see C. Gerschel, these proceedings). The presence of J/ψ suppression in pA collisions, indicates that another physical mechanism is at work. Most authors consider that it consists in the interaction of the pre-resonant $c\bar{c}$ pair with nucleons of the nucleus. A fit of all existing data gives a value of $6 \div 7$ mb for this absorptive cross-section [21]. The same mechanism allows to describe OU and SU collisions but fails to describe the $PbPb$ data –which have a larger (“anomalous”) suppression. The latter has been interpreted as a sign of a deconfining phase transition [21]. However, an alternative explanation has been proposed, based on the idea of comover interactions ($\pi + J/\psi \rightarrow D + \bar{D} + X$) of the same type introduced in the previous section to describe Ω enhancement. It has been shown in [22] that with a cross-section of 0.6 mb one obtains in this way a reasonable description of all the data. At a quantitative level, however, the comover picture tends to slightly overestimate the J/ψ suppression both in central SU and in peripheral $PbPb$ collisions and to underestimate it slightly in very central $PbPb$ collisions. However, this disagreement is rather small (about 2σ). Moreover, there are large uncertainties both in the theory and in the experiment. In particular, recent data on J/ψ production in pA collisions by the E866 collaboration [23] lead to a smaller value of the absorptive cross-section. If these data were confirmed, the agreement of the comover picture would improve. Indeed, by reducing the value of the absorptive cross-section, there would be “more room” for comovers in SU collisions.

The discussion above refers to the true J/ψ over DY data. The NA50 collaboration has also presented the so-called minimum bias (MB) analysis in $PbPb$ collisions. This refers to the ratio

$$\frac{J\psi}{DY} = \left(\frac{J\psi}{MB} \right)_{exp} \times \left(\frac{MB}{DY} \right)_{theory} . \quad (7)$$

Here MB is the single particle inclusive cross-section for charged particles for minimum bias events –i.e. without requiring the presence of a J/ψ or a dimuon pair in the final state. The first factor in the r.h.s. of Eq. (7) has been measured experimentally, while the second one is calculated theoretically. The advantage of this procedure is that the statistic is very

¹ This subject has been discussed in great detail in the lectures by C. Gerschel. The discussion in this paragraph is very sketchy and assumes that the content of her lectures is known.

high (and the statistical errors very small). However, systematic errors do not cancel here.

The ratio obtained in this way shows no saturation at large E_T . On the contrary, it continues to decrease steadily at the highest available values of E_T . This feature cannot be reproduced in a comovers approach, at least in its present version. One has to note, however, that one needs some theoretical assumptions in order to compute the theoretical ratio MB/DY . In particular one assumes that the tail of the E_T distributions of MB and DY are identical. Since both distributions show a very steep fall off at the tail, this assumption plays a very crucial role in the determination of that ratio at very large E_T .

The data [24] can be reproduced in a deconfining scenario [25]. One has to introduce two deconfining phase transitions, a first one for the χ and ψ' and a second one for the direct J/ψ . However, in this approach, the $\langle p_T \rangle$ of the J/ψ versus E_T has a decrease at large E_T which is not seen in the data. On the contrary, the comovers scenario gives a saturation at large E_T both for the ratio J/ψ over DY and for the $\langle p_T \rangle$ of the J/ψ versus E_T (see last paper in [22]).

In conclusion, the present data on J/ψ suppression are very interesting but their interpretation is not yet established. Hopefully, the forthcoming RHIC data will allow to clarify the situation (see section 6).

6. Shadowing corrections and predictions at RHIC and LHC

Using Eq. (3) with $K \sim 2$ at RHIC and $K \sim 3$ at LHC we obtain for central collisions at 7 TeV [26]

$$\frac{dN^{SS}}{dy}(y^* \sim 0) \sim 2000 \quad \frac{dN^{PbPb}}{dy}(y^* \sim 0) \sim 7900 . \quad (8)$$

These results are obtained without taking into account semi-hard collisions (minijets). As discussed in the introduction, the latter do not affect the multiplicities, since the average number of strings is constrained by unitarity. The fact that some of the $q\bar{q}$ strings can be the result of a semi-hard gluon-gluon interaction, will affect the intrinsic p_T of the string ends and, thus, the p_T distribution of produced particles. However, average multiplicities are practically unchanged.

As explained in [26], the values in (8) are upper limits. A reduction in these figures is expected from shadowing corrections. In hard processes, shadowing corrections in the nuclear structure functions are well known. In our approach, however, these corrections are present irrespective of whether the process is hard or soft. Moreover, they have the same physical origin and are governed by the same equations in both cases.

The physical origin of shadowing corrections can be traced to the difference between Glauber model and Gribov field theory. The space-time picture of the interaction is very different in the two cases. Let us consider hadron-nucleus collisions. In the Glauber model, we have successive (billiard ball type of) collisions, while in Gribov theory we have “parallel” collisions of different projectile constituents with target nucleons. A key result of Gribov [27] is that the $h - A$ amplitude can, nevertheless, be written as a sum of multiple-scattering diagrams with elastic intermediate states – which have the same expressions as in the Glauber model. However, in Gribov theory, there are extra multiple-scattering diagrams which contain all possible diffractive excitations of the incoming hadron as intermediate states. At present CERN energies, these extra diagrams lead to corrections to the Glauber formula of the order of $10 \div 20$ % in the total cross-sections. However, their contribution to dN/dy is much larger and leads to a reduction in the figures in (8) by about a factor 2 at RHIC and a factor 3 at LHC [28].

It is well known that the size of high mass excitations of the initial hadron is controlled by triple Pomeron couplings. It has been shown in [29] that the values of the triple reggeon couplings determined from soft diffraction, allow also to describe hard diffraction measured at HERA. It is also well known [30] that the latter determines the size of shadowing effects in the nuclear structure functions at low x . From the analysis in [29] it follows that at a scale $Q^2 \sim 1 \text{ GeV}^2$ and $x \sim 10^{-2}$ (the x -value relevant at RHIC) the shadowing in the Pb structure function leads to its reduction by a factor 0.7. At $x \sim 10^{-3}$ (relevant for LHC) the corresponding reduction is 0.6. Squaring these values (in order to take into account shadowing correction in both projectile and target in the case of $PbPb$ collisions), we obtain the reductions by a factor 2 at RHIC and 3 at LHC as stated above. Similar results are obtained [28] considering that the process is soft and computing the modifications to dN/dy at $y^* \sim 0$ resulting from the extra terms in the Gribov theory –using the standard value of the triple Pomeron coupling.

The above considerations show that the average virtualities relevant for the calculation of the shadowing effects in dN/dy at $y^* \sim 0$ at RHIC and LHC are of the order of 1 GeV^2 . In models where the dominant contribution is semi-hard the relevant average virtualities, obtained from perturbative QCD, are higher and the shadowing effects significantly smaller.

With the above values of dN/dy at $y^* \sim 0$ it is possible to compute the J/ψ suppression at RHIC and LHC resulting from the two mechanisms discussed in section 5, namely nuclear shadowing and comover interaction. The suppression resulting from the former mechanism depends only on the absorptive cross-section which is expected to be the same at all energies. On the contrary, the density of comovers depends strongly on energy and,

as discussed above, on the shadowing effects.

The ratio of J/ψ over DY in a very central $PbPb$ collision at SPS energies over the corresponding ratio in pp collisions obtained in Ref. [22] is 0.23. (This takes into account both nuclear absorption and comovers interaction). Without nuclear shadowing, the corresponding ratios at RHIC and LHC are 0.03 and 10^{-4} , respectively. When shadowing corrections are taken into account the corresponding ratios are significantly larger : 0.11 and 0.02.

7. Event-by-event fluctuations in p_T

Let us define the quantity [31]

$$Z = \sum_{i=1}^N z_i \quad (9)$$

where N is the total number of particles in a single event and

$$z_i = p_{T_i} - \langle p_T \rangle . \quad (10)$$

Here p_{T_i} is the p_T of particle i in the event and $\langle \dots \rangle$ denotes the average over all events. The correlation ϕ is then defined as

$$\phi = \sqrt{\frac{\langle Z^2 \rangle}{\langle N \rangle}} - \sqrt{\langle z^2 \rangle} \quad (11)$$

where $\langle z^2 \rangle$ is determined by mixing particles from different events. In Ref. [31] a simplistic superposition model was considered in which

$$\frac{\langle Z^2 \rangle_{AA}}{\langle N \rangle_{AA}} = \frac{\langle Z^2 \rangle_{NN}}{\langle N \rangle_{NN}} . \quad (12)$$

In this model ϕ is the same in NN and AA . Experimentally, it has been found [32] that ϕ decreases by a factor 3 ÷ 4 from NN to central $PbPb$. This decrease has been interpreted in [31] as a sign of thermalization (see however Ref. [33]).

It turns out that the decrease of ϕ observed experimentally is also reproduced [34] in a Monte-Carlo formulation of the QGSM [4] (a model which is very close to DPM). The rapidity distribution, multiplicity distribution and p_T distribution measured experimentally [32] are also well reproduced by the model [34]. The results for ϕ are [34] : $\phi_{pp} = 9.0$ MeV, $\phi_{PbPb} = 2.4$ MeV at SPS energies and $\phi_{pp} = 76$ MeV, $\phi_{PbPb} = 79$ MeV at RHIC. As we see the values of ϕ predicted at RHIC are much larger than at SPS and practically equal in pp and central $PbPb$.

8. Conclusions

We have shown that the main properties of particle production in hadronic and nuclear collisions can be described in a dynamical string model, the DPM or QGSM. These models do not incorporate non-standard sources of particle production –such as the formation of a thermally equilibrated system or a quark gluon plasma.

The huge stopping observed in central SS and $PbPb$ collisions requires a modification of the model consisting in the introduction of a diquark breaking component. The $PbPb$ data are well reproduced in this way with no extra parameter and predictions for stopping in other systems are obtained. Strange baryon enhancement can also be described in the framework of this improved version of DPM. However, for rare processes such as Ω production (and to a much lesser extent for Ξ production) one has to introduce final state interaction (comovers interaction). This mechanism is also required in order to describe J/ψ suppression. Event-by-event fluctuations in p_T are also well described by the model.

REFERENCES

- [1] G. t’Hooft, Nucl. Phys. **B72**, 461 (1974) ; G. Veneziano, Nucl. Phys. **B74**, 365 (1974).
- [2] DPM : A. Capella, U. Sukhatme, C. I. Tan and J. Tran Thanh Van, Phys. Lett. **B81**, 69 (1979) ; Phys. Rep. **236**, 225 (1994).
- [3] For a review see A. Bialas in Proc. XIIIth Inter. Symp. on Multiparticle Dynamics, ed. by W. Kittle, W. Metzger and A. Stergiou (World Scientific 1983).
- [4] QGSM : A. B. Kaidalov, Phys. Lett. **B116**, 459 (1982). A. B. Kaidalov and K.A. A. Ter-Martyrosyan, Phys. Lett. **B117**, 247 (1982).
- [5] H. G. Dosch, these proceedings.
- [6] G. C. Rossi and G. Veneziano, Nucl. Phys. **B123**, 507 (1997).
- [7] B. Z. Kopeliovich and B. G. Zakharov, Sov. J. Nucl. Phys. **48**, 136 (1988) ; Z. Phys. **C43**, 241 (1989) ; Phys. Lett. **B211**, 221 (1988).
- [8] E. Gotsman and S. Nusinov, Phys. Rev. **D22**, 624 (1980).
- [9] D. Kharzeev, Phys. Lett. **B378**, 238 (1996).
- [10] A. Capella and B. Kopeliovich, Phys. Lett. **B381**, 325 (1996).
- [11] S. E. Vance and M. Gyulassy, nucl-th/9901009.
- [12] A. Capella, E. G. Fereiro and C.A. Salgado, Phys. Lett. **B459**, 27 (1999).
- [13] A. Capella and C.A Salgado, Phys. Rev. C, in press.
- [14] A. Capella, A. B. Kaidalov, A. Kouider-Akil, C. Merino and J. Tran Thanh Van, Z. Phys. **C70**, 507 (1996).

- [15] WA97 collaboration : E. Andersen et al, Phys. Lett. **B433**, 209 (1998) and references therein.
- [16] B. Koch, B. Muller and J. Rafelski, Phys. Rep. **142**, 167 (1986). B. Koch, V. Heinz and J. Pitsut, Phys. Lett. **B243**, 149 (1990).
- [17] S. J. Brodsky and A. H. Mueller, Phys. Lett. **B206**, 685 (1988).
- [18] NA49 collaboration in Proc. Quark Matter 99, Torino, May 1999.
- [19] J. Rafelski, these proceedings.
- [20] T. Matsui and H. Satz, Phys. Lett. **B178**, 416 (1986).
- [21] D. Kharzeev, C. Lourenço, M. Nardi and H. Satz, Z. Phys. **C74**, 307 (1997).
- [22] A. Capella, C. Gerschel and A. Kaidalov, Phys. Lett. **B393**, 431 (1997). N. Armesto and A. Capella, Phys. Lett. **B393**, 431 (1997). N. Armesto, A. Capella and E. G. Ferreira, Phys. Rev. **C59**, 395 (1999).
- [23] E866/Nusea collaboration : M. J. Leitch et al, nucl-exp 9909007.
- [24] NA50 collaboration : M. C. Abreu et al, Phys. Rev. **B410**, 327 (1997) and Proc. Quark Matter 99, ibid.
- [25] M. Nardi and H. Satz, Phys. Lett. **B442**, 14 (1998) ; M. Nardi in Proc. XI Rencontres de Blois, June 1999, Blois, France.
- [26] A. Capella, C. Merino and J. Tran Thanh Van, Phys. Lett. **B265**, 415 (1991).
- [27] V. N. Gribov, JETP **56**, 892 (1969) ; JEPT **57**, 1306 (1969).
- [28] A. Capella, A. Kaidalov and J. Tran Thanh Van, Gribov Memorial Volume of Acta Physica Hungarica (Heavy Ion Physics).
- [29] A. Capella, A. Kaidalov, C. Merino, D. Pertermann and J. Tran Thanh Van, Phys. Rev. **D53**, 2309 (1996).
- [30] A. Capella, A. Kaidalov, C. Merino, D. Pertermann and J. Tran Thanh Van, Eur. Phys. Journ. **C5**, 111 (1998).
- [31] M. Gazdzicki and St. Mrowczynski, Z. Phys. **C54**, 127 (1992).
- [32] NA49 collaboration : H. Appenhauser et al., Phys. Lett. **B459**, 679 (1999).
- [33] St Mrowczynski, Phys. Lett. **B439**, 6 (1998).
- [34] A. Capella, E. G. Ferreira and A. Kaidalov, hep-ph 9903338, Eur. Phys. J. C, in press.

Figure Captions

Fig. 1 : Two string diagram in pp .

Fig. 2 : a) Four string diagram in pp . b) Four string diagram in pA .

Fig. 3 : One string diagram in $\bar{p}p$.

Fig. 4 : Three string diagram in $\bar{p}p$.

Fig. 5 : Three string diagram for the diquark breaking component in pp .

Fig. 6 : Four string diagram for the diquark breaking component in pA .

Fig. 7 : Rapidity distribution of the net baryon number $B - \bar{B}$ in central SS and $PbPb$ collisions. The full (dotted) line is the result with (without) the diquark breaking component.

Fig. 8 : $B + \bar{B}$ yields at mid-rapidities for minimum bias pPb and central $PbPb$ collisions at SPS energies. Full (dashed) lines are the results with (without) final state interaction.

Fig. 9 : Same as Fig. 8 for the ratios \bar{B}/B .

Figure 1

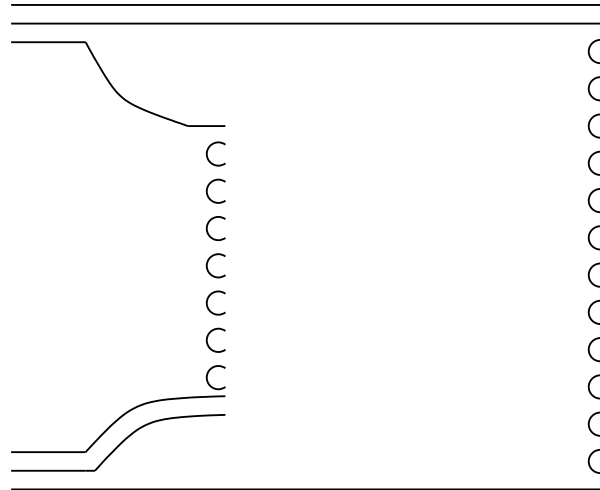


Figure 2

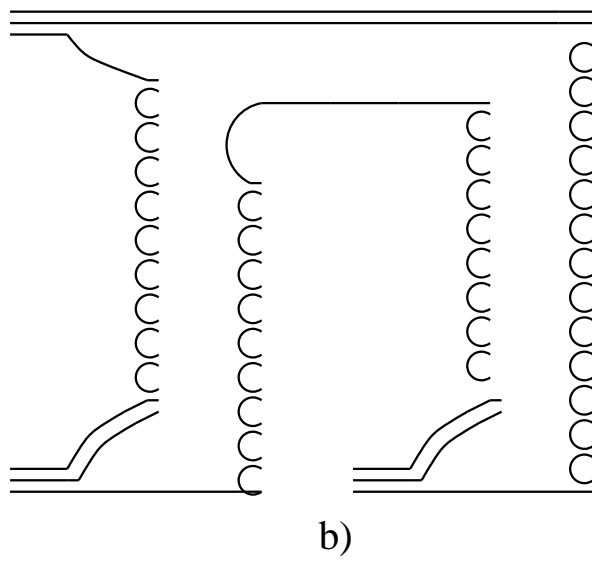
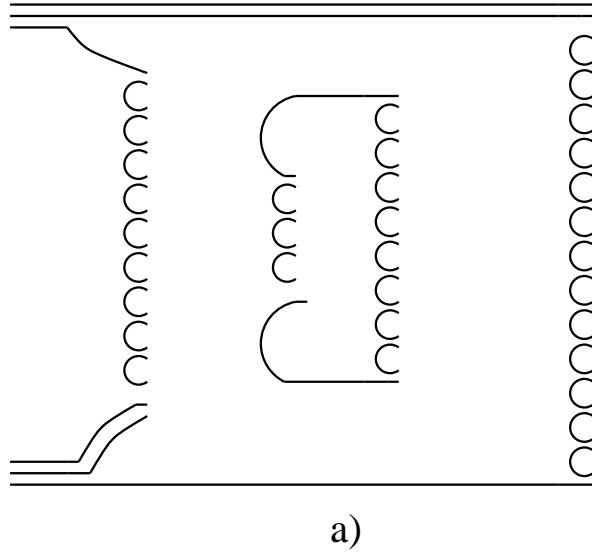


Figure 3

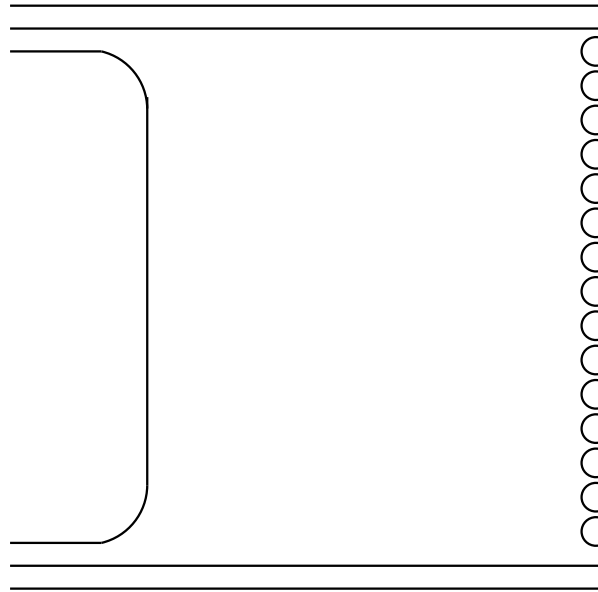


Figure 4

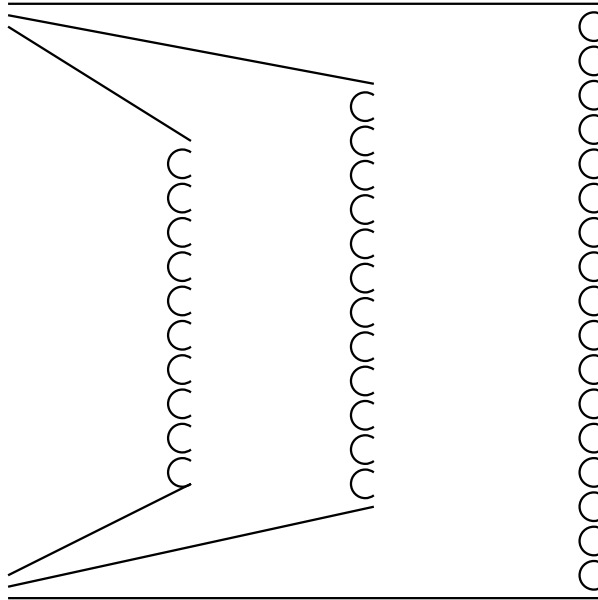


Figure 5

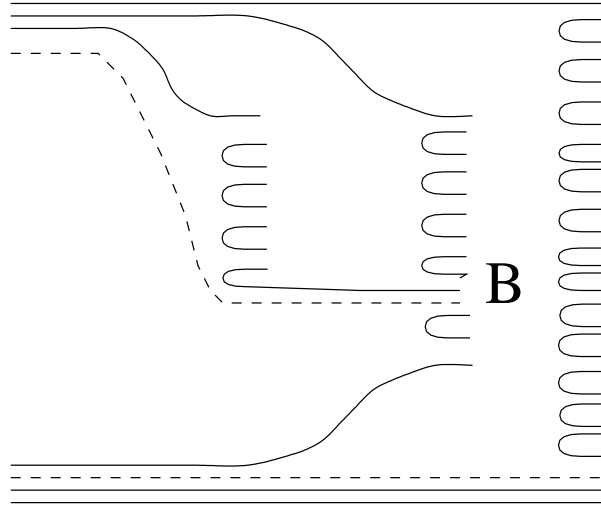


Figure 6

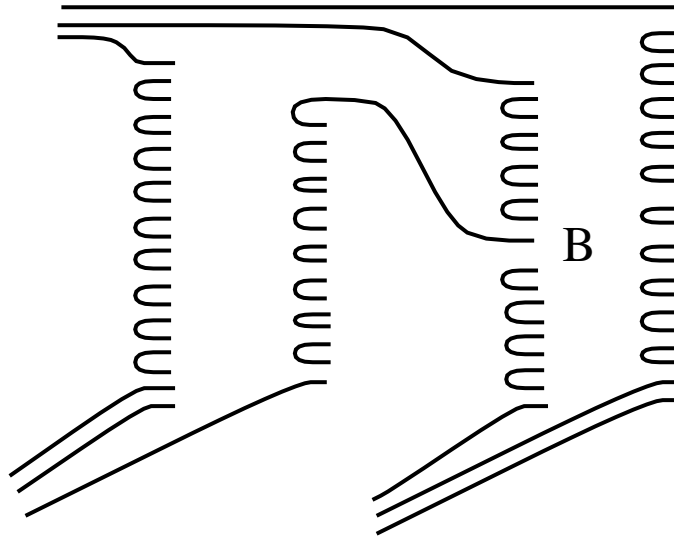


Figure 7

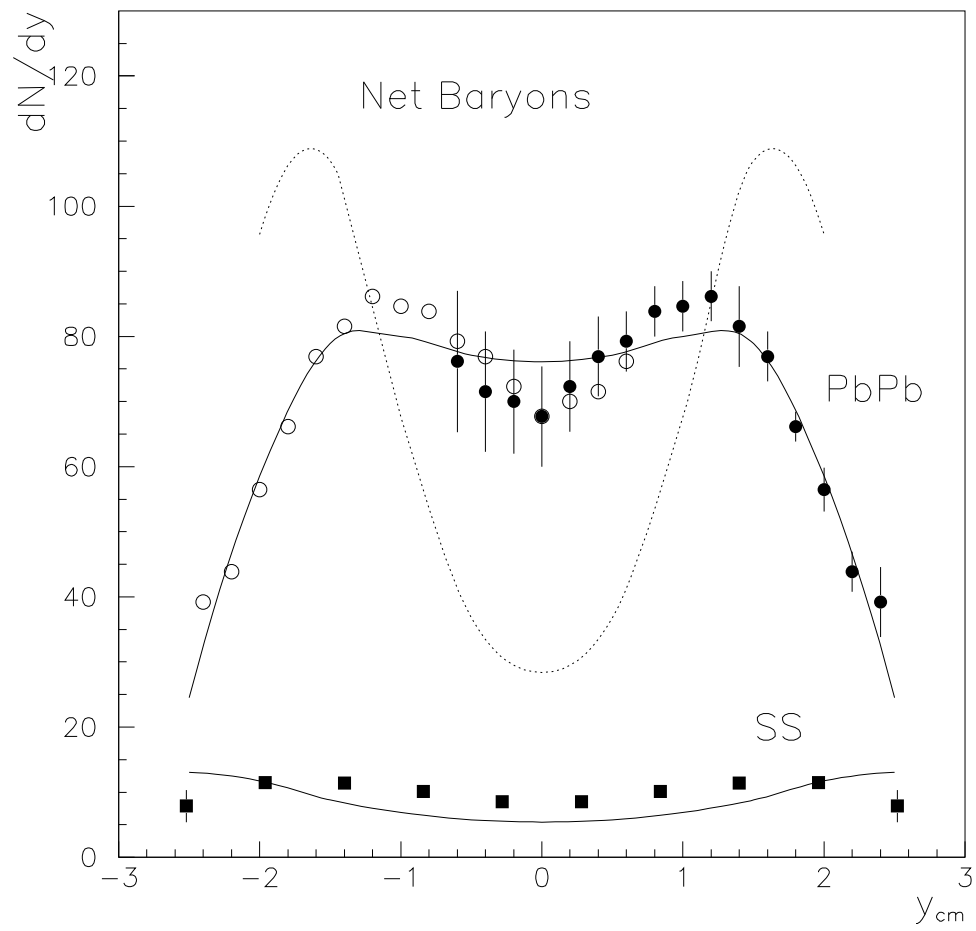


Figure 8

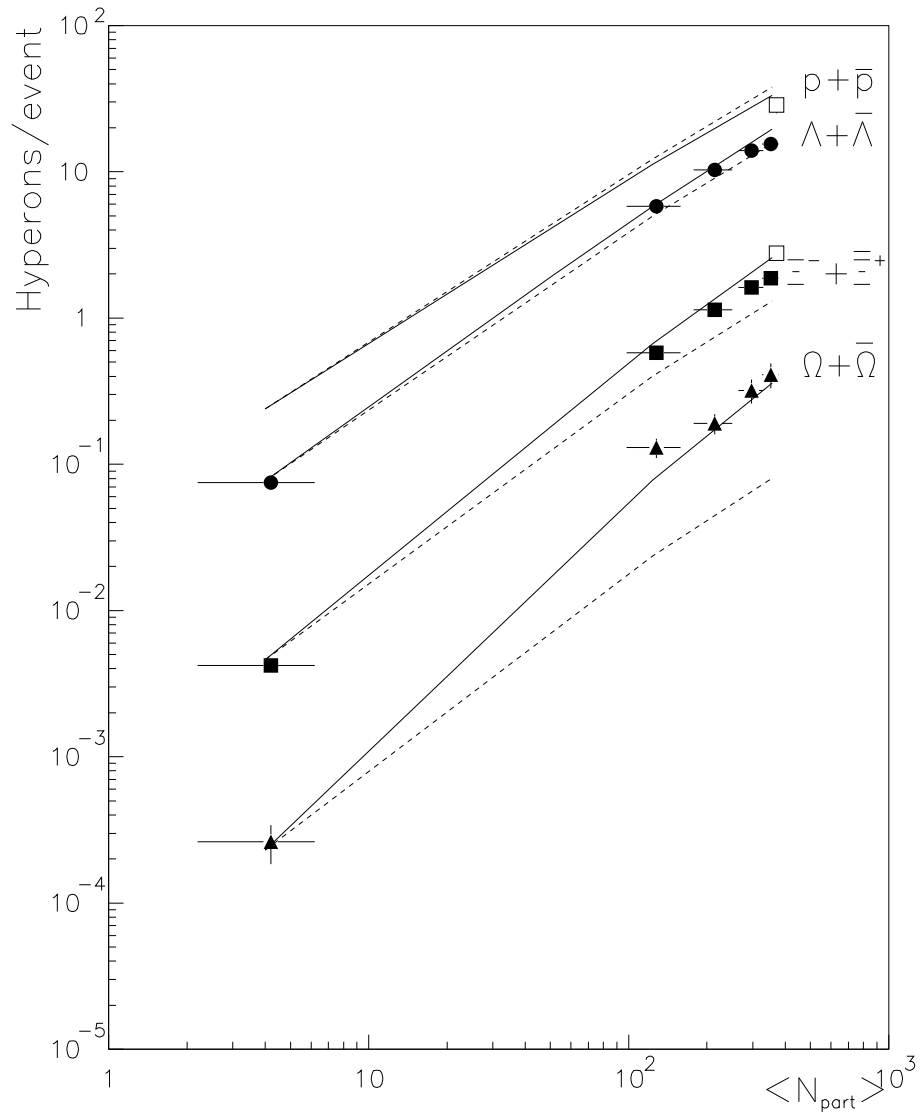


Figure 9

